Internal resonances in a periodic magneto-electro-elastic structure

D. G. Piliposyan, K. B Ghazaryan, and G. T. Piliposian

Citation: Journal of Applied Physics **116**, 044107 (2014); doi: 10.1063/1.4891836

View online: https://doi.org/10.1063/1.4891836

View Table of Contents: http://aip.scitation.org/toc/jap/116/4

Published by the American Institute of Physics

Internal resonances in a periodic magneto-electro-elastic structure

D. G. Piliposyan,[1,a)] K. B Ghazaryan,[1,b)] and G. T. Piliposian[2,c)]
[1]*Department of Dynamics of Deformable Systems and Coupled Fields, Institute of Mechanics, Bagramyan ave 24B, Yerevan 0019, Armenia*
[2]*Department of Mathematical Sciences, The University of Liverpool, M&O Building, L69 7ZL Liverpool, United Kingdom*

(Received 15 May 2014; accepted 21 July 2014; published online 30 July 2014)

Propagation of electro-magneto-acoustic waves in a three phase magneto-electro-elastic periodic structure has been investigated with full coupling between mechanical, electric, and magnetic fields. Due to simultaneous piezoelectric and piezomagnetic effects, an orthogonally polarised electromagnetic wave couples with the similarly polarised lattice vibration, resulting in a both dielectric and magnetic phonon-polaritons. The closed form of dispersion relation has been used to demonstrate the phonon-polariton coupling not only in the long wave region at high acoustic microwave frequencies but also for shorter waves at optical infrared frequencies. The results also show that neither at acoustic nor at optical frequencies the magneto-electro-elastic effect affects the band structure due to the Bragg scattering. © *2014 AIP Publishing LLC*.
[http://dx.doi.org/10.1063/1.4891836]

I. INTRODUCTION

Propagation of electro-magneto-elastic waves in piezoelectric and magneto-electro-elastic (MEE) periodic structures recently attracted much attention due to the wide range of application of these structures in smart materials. It is well known that band gap effects for the propagation of both electromagnetic and acoustic waves can be obtained in such structures. These effects are due to the periodic modulation of the physical parameters resulting in Brag reflection and the formation of frequency band structures. A modulation of dielectric parameters (or refractive indexes) results in photonic crystal with a complete photonic band gap, a frequency range for which the propagation of electromagnetic waves is forbidden.[1] Phononic crystals, on the other, are periodic composites made of two or more materials with different elastic constants and densities and can control the propagation of elastic and acoustic waves.[2–4] The existence of architectures, called phoxonic crystals, simultaneously exhibiting both complete photonic and phononic band gaps has also been discussed,[5] opening the possibility of dual acousto-optic devices.

Bragg reflection, however, may not be the only mechanism for band structure formation. Some other effects such as acousto-optic coupling can also generate band gaps. Analogous to an ionic crystal, where coupling between transverse lattice vibrations and electro-magnetic waves leads to the phonon polariton with possible stop bands in the infrared region,[6,7] piezoelectric and piezomagnetic periodic structures with the periodicity of the lattice expanded from an atomic scale to microns can exhibit similar coupling and resonant band gap structure in the microwave region.[8–10]

In an ionic crystal photon dispersion of EM waves is linear, while phonon dispersion of lattice vibrations is folded, because of the reduced Brillouin zone. The crossing of the photon and optical phonon dispersions takes place in the long-wavelength limit (compared to the periodicity of the lattice) where a strong coupling of the EM wave and the lattice vibration leads to the existence if phonon-polariton gaps.[11] A piezoelectric (PSL) or piezomagnetic (PMSL) superlattice consisting of a periodically domain-inverted dielectric crystal, which has a homogeneous refractive index but periodically modulated piezoelectric or piezomagnetic coefficients, can be considered as a one dimensional diatom chain where the positive and negative ions are arranged periodically. Taking this approach, the phonon-polariton coupling has been investigated in PSL and PMSL in the long-wavelength approximation near the center of the Brillouin zone.[10–13] Theoretical and experimental work has suggested that in a PSL, electro-magnetic waves can also couple with longitudinal superlattice vibrations, introducing a new type of polariton that does not exist in ionic crystals.[14] Therefore, there are not only similarities but also differences between artificial superlattices and real lattices, implying rich physics of artificial microstructures.

While the long-wave approximation only reveals the phonon-photon polariton at high acoustic frequencies in the middle of the Brillouin zone the analytical solution shows that coupling of photons and phonons is possible also at optical frequencies in the whole Brillouin zone.[15–17]

Recently, another kind of superlattice with alternated PE and PM stacks was demonstrated by Zhao *et al.*,[18] where the lattice vibration couples with the EM wave through the piezoelectric effect and piezomagnetic effect, and PE polariton and PM polariton are induced at the same time. However, in these periodic structures, piezoelectric and piezomagnetic phases coupling occurs only through elastic vibrations of the lattice.

In this paper, we investigate the phonon-photon polariton coupling in a new kind of three phase magneto-electro-elastic (MEE) periodic structure with full coupling between mechanical, electric, and magnetic fields. MEE materials are

[a)]davitpiliposyan@mechins.sci.am
[b)]KGhazaryan@mechins.sci.am
[c)]gayane@liv.ac.uk

a class of new composites that consist of simultaneous piezoelectric, piezomagnetic phases and an electro-magnetic coupling coefficient.[19,20] Different problems concerning the frequency band structure of MEE materials due to Bragg scattering have been investigated.[21,22]

In all these studies, the quasi-static approximation is adopted for the electromagnetic field under which both the optical effect and the effect from the rotational part of the electric field are neglected and the acousto-optic resonances have not been investigated. To the best of our knowledge, the full equations of MEE materials in dynamic settings, which can provide accurate formulae for acousto-optic interaction, have not been investigated so far. The solutions for MEE periodic structures will include as particular cases solutions for piezoelectric, piezomagnetic, piezoelectric-piezomagnetic, and piezoelectric-elastic structures.

The analytical dispersion equation will not only allow consideration of phonon polariton coupling in a MEE superlattice with unit cells made of oppositely polarized identical materials, as can be done in the long wave approximation,[10–14] but also allow consideration of such phenomena in phononic/photonic crystals with unit cells made of different constituent materials. We will also be able to investigate phonon-polariton coupling not only in the long-wavelength limit near the center of the Brillouin zone at high acoustic frequencies but also in the whole Brillouin zone closer to optical frequencies.

II. STATEMENT OF THE PROBLEM

We will consider a one dimensional periodic structure composed of two magneto-electro-mechanical (MEE) segments of the same group of symmetry 6 mm with crystallographic axes directed along the Oz direction. The unit cell of a period β consisting of a MEE inclusions of thickness b embedded and perfectly bonded with the matrix made of another MEE material of a thickness a as shown in Figure 1.

A coupled **transverse** electro-magneto-elastic wave travels along the MEE polling direction. The interaction between the **transverse** EM wave and **transverse** elastic waves in each material can be described by the following one-dimensional equations and constitutive relations $(\partial/\partial x, \partial/\partial y = 0)$

$$\frac{\partial \boldsymbol{\sigma}}{\partial z} = \rho \frac{\partial^2 \mathbf{u}}{\partial t^2}, \quad \boldsymbol{\sigma} = G\frac{\partial \mathbf{u}}{\partial z} - e\mathbf{E} - d\mathbf{H}, \tag{1}$$

$$\mathbf{D} = e\frac{\partial \mathbf{u}}{\partial z} + \varepsilon \mathbf{E} + g\mathbf{H}, \quad \mathbf{B} = d\frac{\partial \mathbf{u}}{\partial z} + g\mathbf{E} + \mu \mathbf{H}, \tag{2}$$

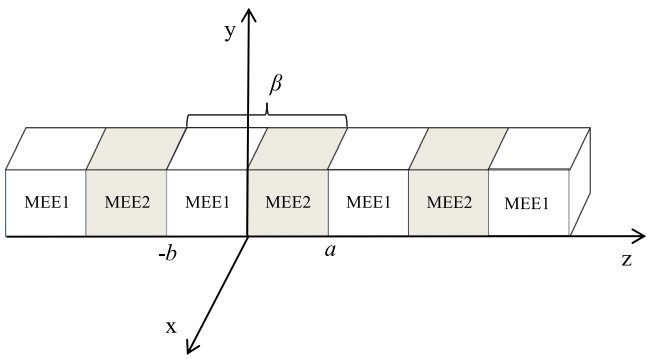

FIG. 1. Schematic diagrams of the 1D periodic MEE structure.

$$\text{rot}\,\mathbf{H} = \frac{\partial \mathbf{D}}{\partial t}, \quad \text{rot}\,\mathrm{E} = -\frac{\partial \mathbf{B}}{\partial t}, \tag{3}$$

where $\mathbf{u} = (u_x, u_y)$, are the displacement vectors, $\boldsymbol{\sigma} = (\sigma_{xz}, \sigma_{yz})$ the stress tensor, $\mathbf{B} = (B_x, B_y)$, $\mathbf{D} = (D_x, D_y)$, $\mathbf{E} = (E_x, E_y)$ and $\mathbf{H} = (H_x, H_y)$ the electric displacement, the electric field intensity and the magnetic induction, magnetic field intensity, ρ, $G = c_{44}$, $\varepsilon = \varepsilon_{11}$ and $\mu = \mu_{11}$ the mass density, the elastic, dielectric and magnetic coefficients, $e = e_{15}$, $d = d_{15}$ and $g = g_{11}$ the piezoelectric, piezomagnetic and electro-magnetic coupling coefficients. After introducing the following notations $u = u_x + \mathrm{i}u_y$, $\sigma(z) = \sigma_{xz}(z) + \mathrm{i}\sigma_{yz}(z)$, $H = H_x + \mathrm{i}H_y$, $\mathrm{E} = E_x + \mathrm{i}E_y$, $D = D_x + \mathrm{i}D_y$, $\mathrm{B} = B_x + \mathrm{i}B_y$, $(\mathrm{i} = \sqrt{-1})$, Eqs. (1)–(3) can be replaced by the system of three equations with respect to unknown functions u, H and E

$$\varepsilon\frac{\partial E}{\partial t} + g\frac{\partial H}{\partial t} - \mathrm{i}\frac{\partial H}{\partial z} + e\frac{\partial^2 u}{\partial z \partial t} = 0, \tag{4}$$

$$g\frac{\partial E}{\partial t} + \mu\frac{\partial H}{\partial t} + \mathrm{i}\frac{\partial E}{\partial z} + d\frac{\partial^2 u}{\partial z \partial t} = 0, \tag{5}$$

$$G\frac{\partial^2 u}{\partial z^2} - \rho\frac{\partial^2 u}{\partial t^2} - e\frac{\partial E}{\partial z} - d\frac{\partial H}{\partial z} = 0. \tag{6}$$

The solutions of Eqs. (4)–(6) can be written as

$$u(z) = m_{11}a_1(z) + m_{13}a_2(z), \quad \sigma(z) = m_{22}b_1(z) + m_{24}b_2(z), \tag{7}$$

$$H(z) = m_{31}a_1(z) + m_{32}b_1(z) + m_{33}a_2(z) + m_{34}b_2(z), \tag{8}$$

$$E(z) = m_{41}a_1(z) + m_{42}b_1(z) + m_{43}a_2(z) + m_{44}b_2(z), \tag{9}$$

where

$$m_{11} = p^2 - \omega^2/c^2, \quad m_{13} = q^2 - \omega^2/c^2 \tag{10}$$

$$m_{22} = c_{44}p^3 - p\tilde{c}_{44}\omega^2/c^2, \quad m_{24} = c_{44}q^3 - q\tilde{c}_{44}\omega^2/c^2, \tag{11}$$

$$m_{31} = p^2 e\omega, \quad m_{32} = p(d\varepsilon - eg)\omega^2, \quad m_{33} = q^2 e\omega, \quad m_{34} = q(d\varepsilon - eg)\omega^2, \tag{12}$$

$$m_{41} = p^2 d\omega, \quad m_{42} = p(e\mu - dg)\omega^2, \quad m_{43} = q^2 d\omega, \quad m_{44} = q(e\mu - dg)\omega^2, \tag{13}$$

and

$$a_1(z) = C_1\exp(\mathrm{i}pz) + C_2\exp(-\mathrm{i}pz),$$
$$b_1(z) = \mathrm{i}(C_1\exp(\mathrm{i}pz) - C_2\exp(-\mathrm{i}pz)),$$
$$a_2(z) = C_3\exp(\mathrm{i}qz) + C_4\exp(-\mathrm{i}qz),$$
$$b_2(z) = \mathrm{i}(C_3\exp(\mathrm{i}qz) - C_4\exp(-\mathrm{i}qz)),$$

$$p = \omega\sqrt{\frac{\xi - \sqrt{\xi^2 - 4}}{2c_0 c}}, \quad q = \omega\sqrt{\frac{\xi + \sqrt{\xi^2 - 4}}{2c_0 c}},$$

$$\xi = \frac{c}{\tilde{c}_0} + \frac{\tilde{c}_0}{c} > 2, \quad \tilde{c}_0 = \sqrt{\frac{\tilde{G}}{\rho}}, \quad c_0 = \sqrt{\frac{G}{\rho}},$$

$$c = \frac{1}{\sqrt{\varepsilon\mu - g^2}}, \quad \tilde{G} = G(1 + r), \quad r = \frac{d^2\varepsilon + e^2\mu - 2deg}{G(\varepsilon\mu - g^2)},$$

where r is the electromagnetic coupling coefficient of the MEE material, C_1, C_2, C_3, C_4 are complex constants.

Equations (4)–(6) couple transverse elastic displacements with transverse components of the electromagnetic field. The phase velocity of the coupled waves can be determined from Eq. (22).

For a piezoelectric material ($d = 0$, $g = 0$), complex equations (4)–(6) uncouple into two sets of identical equations describing coupled transverse electromagnetic and elastic waves of different modes (u_x, E_x, H_y) and (u_y, E_y, H_x). For a piezomagnetic material ($e = 0$, $g = 0$), Eqs. (4)–(6) uncouple into two identical set of equations describing coupled transverse electromagnetic and elastic waves of different modes (u_x, E_y, H_x) and (u_y, E_x, H_y). These independent modes can be set in motion by perturbing the external electromagnetic or elastic fields.

For writing interface and Bloch boundary conditions, it is convenient to introduce the following two vectors $\tilde{\boldsymbol{U}}(z) = (u, \sigma, H, E)^T$, $\boldsymbol{A}(z) = (a_1, b_1, a_2, b_2)^T$ and the matrix $M = \{m_{ij}\}$ with nonzero elements (10)–(13) ($m_{12} = m_{14} = m_{21} = m_{23} = 0$) and write Eqs. (7)–(9) as

$$\tilde{\boldsymbol{U}}^{(s)}(z) = M^{(s)}\boldsymbol{A}^{(s)}(z), \tag{14}$$

where superscripts $s = 1, 2$ and here and elsewhere show that the functions belong to the mediums 1 and 2. The interface and Bloch conditions can then be written as

$$\tilde{\boldsymbol{U}}^{(1)}(0) = \tilde{\boldsymbol{U}}^{(2)}(0), \quad \tilde{\boldsymbol{U}}^{(1)}(-b) = \lambda\tilde{\boldsymbol{U}}^{(2)}(a), \tag{15}$$

where $\lambda = e^{ik\beta}$ and k is the Bloch wave number.

The interface conditions represent continuity conditions for the displacements, shear stresses and tangential components of the magnetic and electric field vectors (tangent to interface surfaces). We also need the transfer matrix within a homogeneous material which for each MEE material has the form[14]

$$T(z) = \begin{pmatrix} C_p & S_p & 0 & 0 \\ -S_p & C_p & 0 & 0 \\ 0 & 0 & C_q & S_q \\ 0 & 0 & -S_q & C_q \end{pmatrix},$$

where $C_p = \cos(pz)$, $S_p = \sin(pz)$, $C_q = \cos(qz)$, $S_q = \sin(qz)$. Using the property of the transverse matrix $\boldsymbol{A}^{(s)}(z') = T^{(s)}(z' - z)\boldsymbol{A}^{(s)}(z)$ and the Bloch-Floquet conditions we arrive at the following matrix eigenvalue problem:

$$(S - \lambda \mathrm{I})\boldsymbol{A}^{(2)}(-b) = 0, \tag{16}$$

where $\mathrm{S} = (M_2T^{(2)}(a)M_2^{-1})(M_1T^{(1)}(-b)M_1^{-1})$, and the following dispersion equation holds:

$$F(\lambda, \omega) = \lambda^4 + f(\omega)\lambda^3 + g(\omega)\lambda^2 + f(\omega) + 1 = 0, \tag{17}$$

where the expressions for f and g for an MEE superlattice are given in the Appendix. Presenting Eq. (17) in the form

$$\left(\lambda + \frac{1}{\lambda}\right)^2 + \left(\lambda + \frac{1}{\lambda}\right)f + g - 2 = 0, \tag{18}$$

and taking into account that $\lambda = e^{ik\beta}$ and $\lambda + \lambda^{-1} = 2\cos\beta k$ the trigonometric solution of the dispersion equation is

$$\cos\beta k = \frac{1}{4}\left(-f + \sqrt{f^2 - 4g + 8}\right),$$
$$\cos\beta k = \frac{1}{4}\left(-f - \sqrt{f^2 - 4g + 8}\right). \tag{19}$$

Dispersion equations (19) describe not only the band structure at both acoustic and optic frequencies due to the Bragg scattering but also band gaps due to acousto-optic resonances. As a particular case this setting will also allow us to study periodic structures with alternating layers of piezoelectric, piezomagnetic or piezoelectric and piezomagnetic materials with different polarizations and different mechanical properties.

Without piezoelectric-piezomagnetic coupling equations (19) uncouple to give a dispersion equation for the propagation of a pure electromagnetic wave

$$\cos(\beta k) = \cos\left(\frac{a\omega}{c^{(1)}}\right)\cos\left(\frac{a\omega}{c^{(2)}}\right) - \frac{1}{2}\left(\frac{Z_{op}^{(1)}}{Z_{op}^{(2)}} + \frac{Z_{op}^{(2)}}{Z_{op}^{(1)}}\right)\sin\left(\frac{a\omega}{c^{(1)}}\right)\sin\left(\frac{a\omega}{c^{(2)}}\right) \tag{20}$$

and pure acoustic wave

$$\cos(\beta k) = \cos\left(\frac{a\omega}{c_0^{(1)}}\right)\cos\left(\frac{a\omega}{c_0^{(2)}}\right) - \frac{1}{2}\left(\frac{Z_{ac}^{(1)}}{Z_{ac}^{(2)}} + \frac{Z_{ac}^{(2)}}{Z_{ac}^{(1)}}\right)\sin\left(\frac{a\omega}{c_0^{(1)}}\right)\sin\left(\frac{a\omega}{c_0^{(2)}}\right), \tag{21}$$

in the periodic structures where

$$Z_{op}^{(j)} = \sqrt{\mu^{(j)}/\varepsilon^{(j)}}, \quad Z_{ac}^{(j)} = \sqrt{G^{(j)}\rho^{(j)}}, \quad j = 1, 2,$$

are optic and acoustic impedances in two materials.

For a non-periodic MEE material, the dispersion equation (17) describes two magneto-electro-acoustic waves given by the dispersion equation

$$\left(1 - (\varepsilon\mu - g^2)\frac{\omega^2}{k^2}\right)\left(1 - \frac{\rho}{G}\frac{\omega^2}{k^2}\right) = \frac{r\omega^2(\varepsilon\mu - g^2)}{k^2}. \tag{22}$$

To a first degree approximation for $r \ll 1$ Eq. (22) gives two solutions, one describing a quasi-acoustic wave $\omega^2/k^2 \approx c_0^2(1 - rc_0^2/c^2)$ and the other a quasi-electromagnetic wave $\omega^2/k^2 \approx c^2(1 + rc_0^2/c^2)$. Due to the magneto-electro-elastic coupling, the phase velocity of the first wave is lower than the acoustic wave velocity and the velocity of the second wave is greater than that of the electromagnetic wave. The two dispersion curves are straight lines passing through the origin and not exciting frequency band gaps or acousto-optic coupling.

III. NUMERICAL RESULTS AND DISCUSSION

A. Phonon-polariton at acoustic frequencies

Two dispersion curves in Eq. (19) describe the band structure due not only to Bragg scattering but also internal resonances occurring from interactions between electromagnetic and acoustic waves. These interactions in MEE

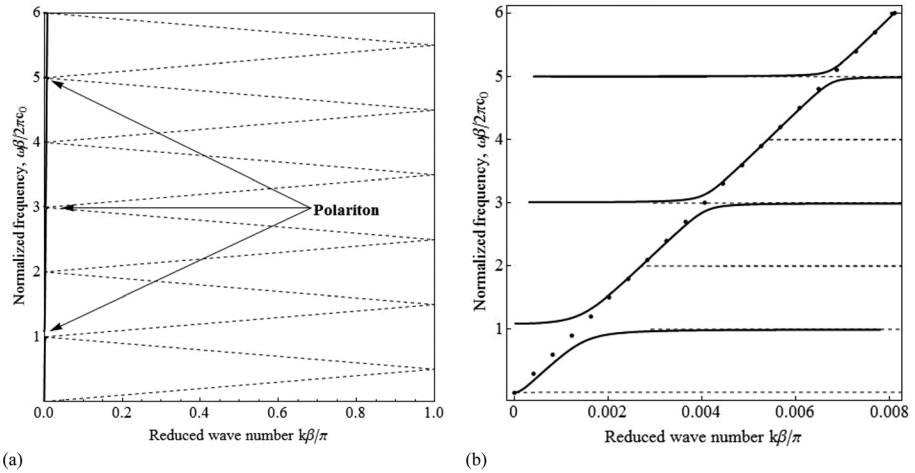

FIG. 2. (a) Band structure of an MEE superlattice at acoustic frequencies for $a=b$, (b) the zoomed profile of the band structure and phonon-polariton near the centre of the Brillouin zone. The horizontal dashed lines correspond to the phase velocity of the acoustic wave enhanced by the piezoelectric-piezomagnetic coupling. The linear oblique dotted line corresponds to the phase velocity of a pure EM wave.

periodic crystals at acoustic frequencies give rise to polariton behavior at wavelengths much larger than the cell length that is not associated with Bragg scattering but rather the acousto-**optic** coupling near resonance frequencies. For piezoelectric superlattices, these interactions at high acoustic frequencies have been investigated in a long wave approximation for different polarizations.[8–14] The analytical expression of the dispersion equations (19) describes acousto-optic coupling not only in the long wave region but also in the whole Brillouin zone at **optic** frequencies which cannot be shown in the long wave approximation approach.

The analysis of Eq. (19) shows that at acoustic frequencies ($\omega \sim c_0\beta^{-1}$) as $k_0\beta \to 0$ there is an interaction between the quasi-electromagnetic wave described by Eq. (20) and the quasi-acoustic wave described by Eq. (21). When the frequencies of these waves and wave numbers nearly coincide this interaction results in coupling and creation of two dispersion curves, low and high polaritons, separated by polariton band gaps. The size of the band gaps depends on material constants and the configuration of the MEE superlattice.

Numerical calculation have been carried out both at acoustic and optic frequency regions for a MEE superlattice and MEE phononic crystal made of two different constituent materials. Material parameters of the MEE periodic crystal $BaTiO_3$–$CoFe_2O_4$ for different volume fractions are taken from Yu *et al.*[23]

Since the dispersion curve of photons at acoustic frequencies is too close to the vertical axis (Fig. 2(a)) the coupling between the EM wave and superlattice vibration can be seen in the long wavelength region. Figure 2(b) shows the acousto-optic resonance in the MEE superlattice which is made of the same MEE material with opposite polarizations in two adjacent domains. Although in this case the MEE structure can have frequency band gaps due to the Bragg scattering, which in the case of a piezoelectric superlattice with the wave vector orthogonal to the polling direction has been shown in Piliposian *et al.*,[15] in the present setting when the wave vector of a coupled wave is parallel to the polling direction the magneto-electro-coupling effect is quite week so that it even is not present in the equations in a quasistatic setting. That is why band gaps at the end of the Brillouin zone are nonexistent for a MEE superlattice (Fig. 2(a)) and negligible for a periodic crystal having two different constituent materials in the unit cells with small differences in their impedances. (Fig 3(a)). However, the detailed profile of the band structure in the long wavelength region in Figure 2(b) demonstrates the phonon-photon coupling. The horizontal lines correspond to the phase velocity of the acoustic wave enhanced by the piezoelectric-piezomagnetic coupling. The linear oblique dotted line computed by Eq. (20) corresponds to the phase velocity of **a** pure EM wave uncoupled to the lattice vibrations. The region of crossover of these two lines

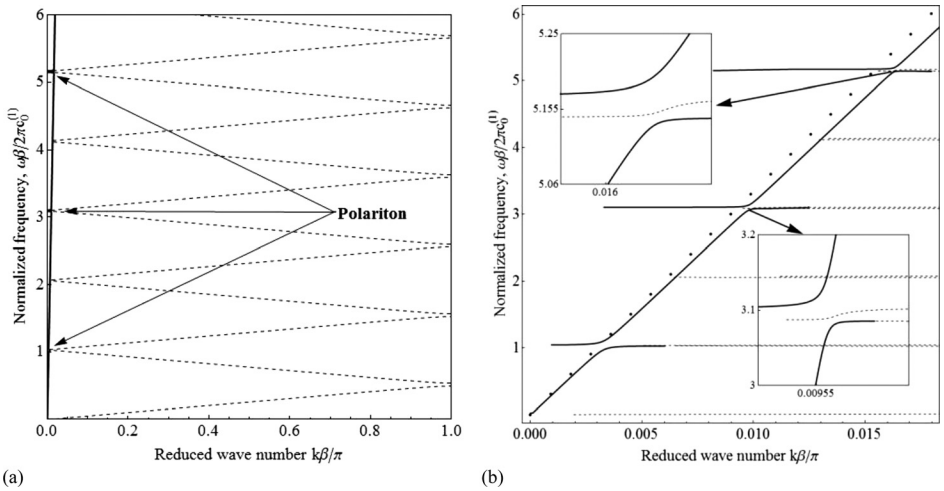

FIG. 3. (a) Band structure of the MEE periodic structure at acoustic frequencies for $a=b$, (b) the zoomed profile of the band structure and phonon-polariton near the centre of the Brillouin zone. The horizontal dashed lines correspond to the phase velocity of the acoustic wave enhanced by the piezoelectric-piezomagnetic coupling. The linear oblique dotted line corresponds to the phase velocity of a pure EMwave.

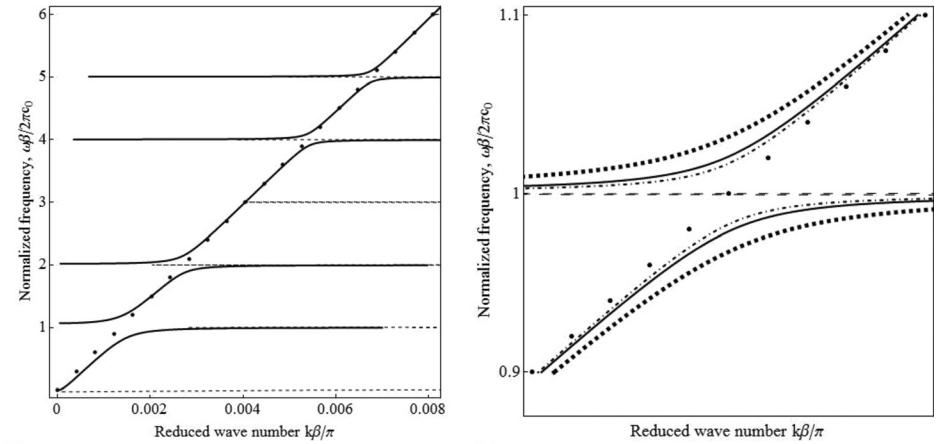

FIG. 4. (a) The phonon-polariton band structure of the MEE superlattice at acoustic frequencies near the centre of the Brillouin zone for $a = 2b$, (b) the inner dot-dash line shows the phonon-polariton band gap, the bold line is the gap for a doubled value of the piezomagnetic coefficient, the outer dot lines show the gap for doubled value of a piezoelectric coefficient. The horizontal dashed lines correspond to the phase velocity of the acoustic wave enhanced by the piezoelectric-piezomagnetic coupling. The linear oblique dotted line corresponds to the phase velocity of a pure EM wave.

is the resonance region, where for a very narrow range of k neither an EM nor an acoustic wave can propagate.

As it shows in Figure 2(b), the acousto-optic coupling for $a = b$ takes place at not all integer multiples of fundamental resonance frequency but only for odd values $(\omega\beta)/(2\pi c_0^{(1)}) = m$, $m = 1, 3, \ldots$, for even m polariton is not excited. For $a = 2b$, polaritons are not excited with threefold order of the values m (Fig. 4(a)). The same phonon-polariton features can be seen also for a periodic MEE structure with different constituent materials (Fig. 3(b)). In both cases, low order polaritons have larger gaps which get narrower for high order polaritons. For an MEE superlattice, the width of the first gap is about 7.5%, higher than for piezoelectric superlattices.[9,12] However as Figure 3(b) shows the widths of polariton gaps can be changed by changing the magneto-electro-mechanical coupling coefficient r, with piezoelectric coefficient having a stronger impact on the phonon-polariton gap than the piezomagnetic coefficient (Fig. 4(b)). If the period in the periodic MEE structure is 4.5 μm, then the first polariton gap will be excited close to a resonance frequency 2 GHz and the second around a resonance frequency 6 GHz which lie at microwave region.

B. Phonon-polariton at optic frequencies

The explicit expression of dispersion equations (19) normalised with the "speed" of the EM wave $c = 1/\sqrt{\varepsilon\mu - g^2}$ demonstrates magneto-acoustic coupling also at optic frequencies. In this resolution, Eq. (19) fills the whole space with the interface line coinciding with the line described by Eq. (20) (Fig. 5(a)). The enlarged Figures 5(b), 6(a), and 6(b) in resolution of the acoustic frequency each around one particular point on the interface line for a MEE superlattice clearly show polariton gaps at optic frequencies. The acousto-optic resonances here occur for short waves, unlike phonon polaritons at acoustic frequencies.

The phonon-polariton coupling occurs also for an MEE periodic structure made of different constituent materials (Fig. 7(a)). The enlarged picture near the marked points in Fig. 7(a) shows a phonon-polariton gap at different optic frequencies (Figs. 7(b) and 8). If the period in the periodic MEE structure is 4.5 μm, then the first polariton gap will be excited close to a resonance frequency 2.01 THz and the second around a resonance frequency 4.02 THz which lie at the infrared region.

In this case, the structure also acts as a photonic crystal showing band gaps at the end of the Brillouin zone due to a periodic modulation of the refractive indexes.

IV. CONCLUSION

We have calculated a closed form of the dispersion relation for the propagation of coupled electro-magneto-elastic waves in a three phase magneto-electro-elastic (MEE) periodic structure. This is a new class of composites consisting of piezoelectric and piezomagnetic phases with both elastic and magneto-electric coupling between the phases. Due to

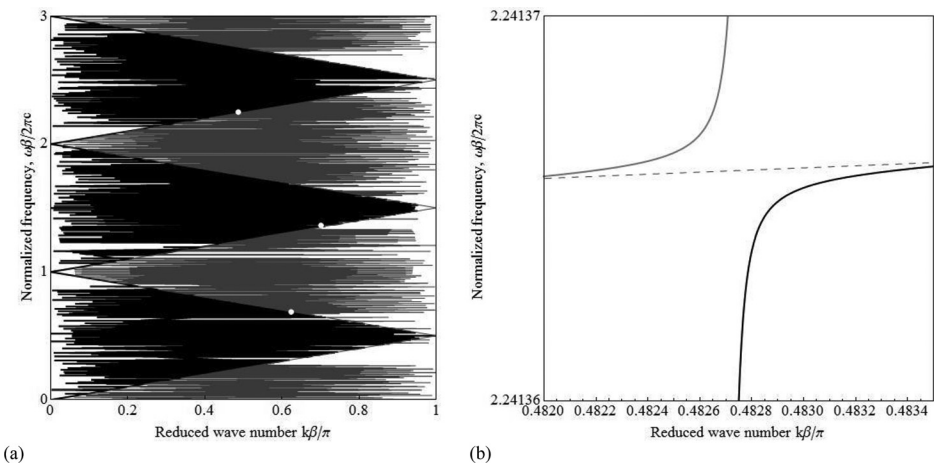

FIG. 5. (a) Band structure of the MEE superlattice at optic frequencies and (b) the zoomed profile of the band structure near $k\beta/\pi = 0.4$.

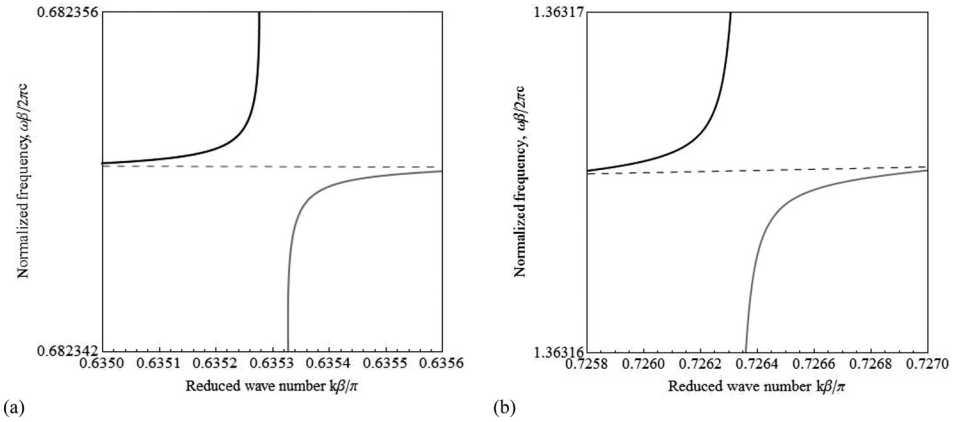

FIG. 6. The zoomed profile of the band structure near (a) $k\beta/\pi = 0.6$ and (b) $k\beta/\pi = 0.7$ of a MEE periodic superlattice at **optic** frequencies.

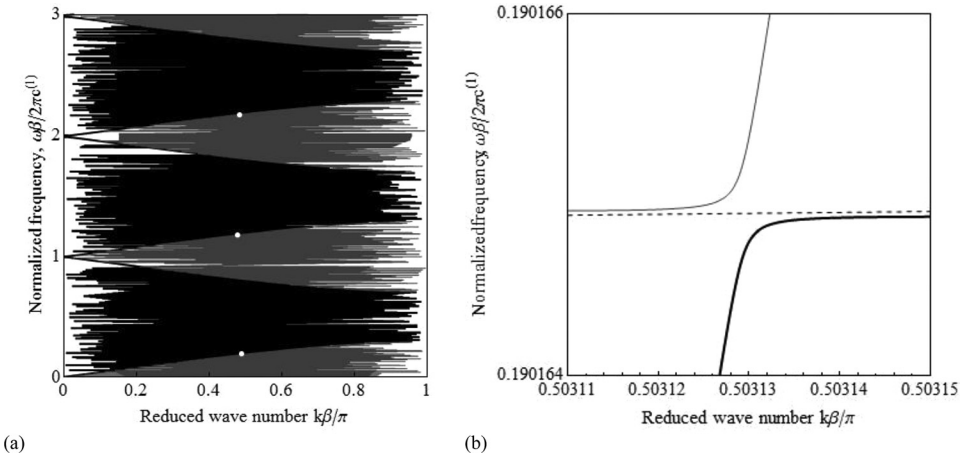

FIG. 7. (a) Band structure of the MEE periodic structure at optic frequencies and (b) the zoomed profile of the polariton dispersion curves near $k\beta/\pi = 0.5$.

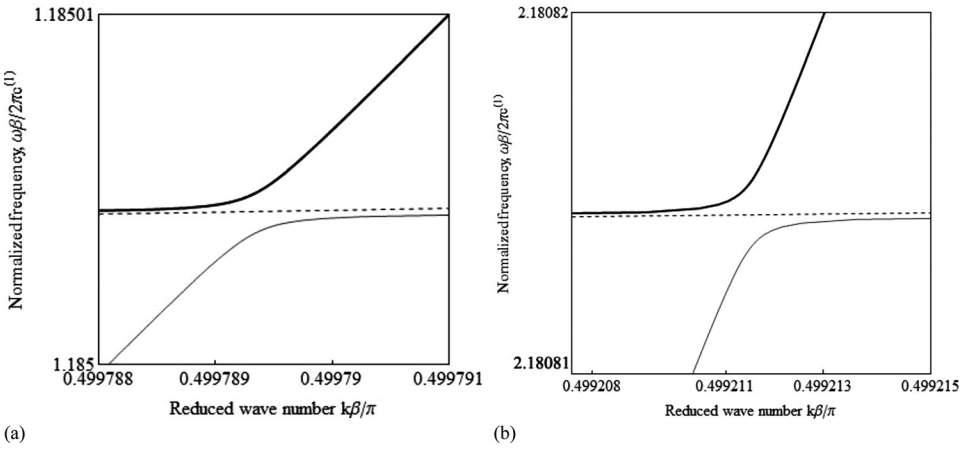

FIG. 8. (a) and (b) the zoomed profile of the polariton dispersion curves near $k\beta/\pi = 0.5$ at different **optic** frequencies.

the dynamic settings of the Maxwell's equations, both the **optic** effects and effects from the rotational part of the electric field are taken into account, giving an opportunity to analyse the acousto-optic resonances. These resonances give rise to phonon-photon polaritons at acoustic (in a microwave region) and **optic** frequencies (in infrared region).

In the present setting when the wave vector of a magneto-electro-elastic coupled wave is parallel to the polling direction, the piezoelectric, piezomagnetic and magneto-electric effects on frequency band gaps due to Bragg scattering are quite weak. In a quasistatic setting of the Maxwell's equations, the piezoelectric and piezomagnetic coefficients are even not present in the equations. The acousto-optic coupling however due to piezoelectric, piezomagnetic and magneto-electric effects is strong. At high acoustic frequencies this coupling creates phonon-polariton gaps in the middle of the Brillouin zone. At **optic** frequencies phonon-polariton coupling occurs throughout the whole Brillouin zone.

In a following paper, our next step will be to use the long wave approximation applied to a MEE superlattice structure to investigate the permittivity and permeability functions near the acousto-optic resonance regions, including the possibility of simultaneous negative regions for these functions to form a so called "left–handed" material.

ACKNOWLEDGMENTS

This research was supported by The Royal Society International Travel Grant 51306 and State Committee of Science of Armenia Grant No. SCS 13-2C005.

APPENDIX: EXPRESSIONS FOR FUNCTIONS G AND F IN EQUATION (17)

$$\begin{aligned} g = V[&3(4+\xi^2)+48(1+r)^2\alpha^8(4+\xi^2)-8\alpha^2\xi w_1 w_2 \\ &+2\alpha^4(8(8+5r(2+r))+2(22+r(26+r))\xi^2+3\xi^4) \\ &-4r^2\alpha^4(\xi^2-4)\cos(aq)+\cos(ap)(4r^2\alpha^4(4-\xi^2) \\ &-(3(4+\xi^2)+48(1+r)^2\alpha^8(4+\xi^2)-8\alpha^2\xi w_1 w_2 \\ &+4\alpha^4(8+4r(10+7r)+(34-(r-26)r)\xi^2))\cos(aq)) \\ &+16(w_2-(2+r)\alpha^2\xi)(2(\xi-4(1+r)\alpha^2)(\alpha^2\xi-1) \\ &+2(\xi w_2-4(2+r)\alpha^2)\cos(ap)\cos(aq))\sin(ap)\sin(aq)], \end{aligned}$$

$$\begin{aligned} f = -V(\xi^2-4)[&2(w_2-2\alpha^2\xi)^2+(1-4(1+r)\alpha^4)^2\cos(aq) \\ &+(1-4(1+r)\alpha^4)^2-4(1+4\alpha^4(3+w_2)-2\alpha^2 w_2\xi) \\ &\times\cos(aq))\cos(ap)+32\alpha^2(w_2-(2+r)\alpha^2\xi) \\ &\times\sin(ap)\sin(aq)], \end{aligned}$$

$$V=\frac{1}{2\alpha^4\left(\xi^2-4\right)^2},\quad \alpha=\frac{c_0}{c},\quad w_1=\left(8+6r+\xi^2\right),$$
$$w_2=1+4(1+r)\alpha^4.$$

[1]E. Yablonovitch, Phys. Rev. Lett. **58**, 2059 (1987).
[2]M. M. Sigalas and E. N. Economou, J. Sound Vib. **158**, 377 (1992).
[3]J. O. Vasseur, P. A. Deymier, B. Chenni, B. Djafari-Rouhani, L. Dobrzynski, and D. Prevost, Phys. Rev. Lett. **86**, 3012 (2001).
[4]M. S. Kushwaha, P. Halevi, G. Martínez, L. Dobrzynski, and B. Djafari-Rouhani, Phys. Rev. B **49**, 2313 (1994).
[5]M. Maldovan and E. L. Thomas, Appl. Phys. B **83**, 595–600 (2006).
[6]K. Huang, Proc. R. Soc. A **208**, 352 (1951).
[7]C. Huang and Y. Zhu, AIP Adv. **2**, 042117 (2012).
[8]C. P. Huang and Y. Y. Zhu, Phys. Rev. Lett. **94**, 117401 (2005).
[9]W. Zhang, Z. Liu, and Z. Wang, Phys, Rev. B **71**, 195114 (2005).
[10]H. Liu, S. N. Zhu, Z. G. Dong, Y. Y. Zhu, Y. F. Chen, N. B. Ming, and X. Zhang, Phys. Rev. B **71**, 125106 (2005).
[11]X. J. Zhang, R. Q. Zhu, J. Zhao, Y. F. Chen, and Y. Y. Zhu, Phys. Rev. B **69**, 085118 (2004).
[12]M. Y. Yang, L. C. Wu, and J. Y. Tseng, Phys. Lett. A **372**, 4730 (2008).
[13]Z. Liu and W. Zhang, J. Phys. Condens. Matter **18**, 9083 (2006).
[14]Y. Y. Zhu, X. J. Zhang, Y. Q. Lu, Y. F. Chen, S. N. Zhu, and N. B. Ming, Phys. Rev. Lett. **90**, 053903 (2003).
[15]G. T. Piliposian, A. S. Avetisyan, and K. B. Ghazaryan, Wave Motion **49**, 125 (2012).
[16]D. G. Piliposyan, K. B. Ghazaryan, and G. Piliposian, Ultrasonics **54**, 644 (2014).
[17]Y. Xu, C. Chen, and X. Tian, Phys. Lett. A **377**, 895 (2013).
[18]J. Zhao, R. Yin, T. Fan, and N. Ming, Phys. Rev. B **77**, 075126 (2008).
[19]A. K. Soh and J. X. Liu, J. Intell. Mater. Syst. Struct. **16**, 597 (2005).
[20]J. Lee, J. G. Boyd, and D. C. Lagoudas, Int. J. Eng. Sci. **43**, 790 (2005).
[21]Y. Wang, F. Li, K. Kishimoto, Y. Wang, and W. Huang, Wave Motion **46**, 47 (2009).
[22]J. F. Robillard, O. B. Matar, J. O. Vasseur, P. A. Deymier, M. Stippinger, A. C. Hladky-Hennion, Y. Pennecand, and B. Djafari-Rouhani, Appl. Phys. Lett. **95**, 124104 (2009).
[23]H. Yu, L. Wu, and H. Li, Int. J. Solid Str. **51**, 336 (2014).